Experimental evaluation of micromorphic elastic constants in foams and lattices

R. S. Lakes

September 12, 2023

Preprint, R. S. Lakes, Experimental evaluation of micromorphic elastic constants in foams and lattices, Zeitschrift fur angewandte Mathematik und Physik (ZAMP), 74, Article number: 31 (2023). https://doi.org/10.1007/s00033-022-01923-5

Abstract

Micromorphic (microstructure) elastic constants are considered within the context of experimental results for foams and rib lattices, and of subsets such as Cosserat elasticity, void elasticity and reduced micromorphic elasticity. Experimentally, longitudinal wave dispersion and cut off frequencies reveal several of the micromorphic b coefficients. In static experiments, no size effects are evident in compression for the materials studied. The corresponding micromorphic a coefficients are not distinguishable from zero. By contrast, Cosserat effects are pronounced in these materials.

1 Introduction

Classical elasticity is not the only theory of elasticity. Classical elasticity incorporates the displacement of points from which one determines strain, and force per area or stress. For isotropic materials there are two independent elastic constants [1]. If one allows couple stress (a torque per unit area) associated with deformation gradients, the couple stress theory, with four independent isotropic elastic constants is obtained [3]. The Cosserat theory of elasticity [4] [5] [6] includes a local rotation or micro-rotation of points in addition to the translation of points in classical elasticity. Cosserat elasticity incorporates a couple stress as well as the usual stress; there are six isotropic elastic constants. Cosserat freedom in materials is well established experimentally. Cosserat elasticity with a local inertia term is called micropolar elasticity [7]. The microstructure theory of Mindlin [8], also called micromorphic elasticity, is more general than Cosserat elasticity. It allows the points in the continuum to translate, rotate and deform; there are 18 elastic constants for isotropic solids. Some other particular cases of microstructure elasticity have been developed. If one incorporates a local dilatation variable as is done in void elasticity [9], there are 5 elastic constants. A theory with a combination of a dilatation variable with the rotation variable of Cosserat elasticity is called microstretch elasticity [10]. A relaxed micromorphic elasticity [11] incorporates some micromorphic freedom as well as the freedom of Cosserat elasticity. theory contains two additional elastic constants for a total of 8. In all these generalized continuum theories characteristic lengths can be expressed as the square root of a ratio of one or more nonclassical constants to a classical modulus.

Lattices of ribs have been analytically homogenized to predict Cosserat constants [12] [13]. Characteristic lengths were considerably smaller than the cell size. Composites with stiff spheres in a soft matrix were shown by homogenization analysis to have characteristic lengths of zero [14]. Chiral two dimensional rib lattices with negative Poisson's ratio [15] were predicted to have a Cosserat characteristic length [16] on the order of the cell size. Crystal lattices have been analyzed as Cosserat

continua [17] and as micromorphic continua [18] and results compared with prior observations of phonon dispersion. We remark that a simplified micromorphic plasticity model was used to predict stress concentration effects in metal foam [19]. A characteristic length for plasticity and a characteristic length for fracture were determined. In the present context we consider linear elastic response, not plasticity. Experimental results for generalized continuum response are reviewed below.

In this research, static and dynamic methods for determining micromorphic elastic constants are presented and compared. Experimental results via both methods are presented and compared.

2 Theory

2.1 Microstructure / micromorphic elasticity

In microstructure elasticity [8], also called micromorphic elasticity, the points in the continuum translate, rotate and deform. A micro-deformation ψ_{ij} is defined such that the symmetric part $\psi_{(ij)} = \frac{1}{2}(\psi_{ij} + \psi_{ji})$ is the micro-strain and the antisymmetric part $\psi_{[ij]} = \frac{1}{2}(\psi_{ij} - \psi_{ji})$ is the micro-rotation. As in the Cosserat theory, the micro-rotation differs from the macro-rotation $r_i = (e_{ijk}u_{k,j})/2$ which depends on gradients of displacement; e_{ijk} is the permutation symbol. The small strain tensor is $\epsilon_{ij} = \frac{1}{2}(u_{i,j} + u_{j,i})$ in which u_i the displacement vector. It is called the macro-strain to distinguish it from the micro-strain. The relative deformation γ_{ij} is defined as $\gamma_{ij} = \frac{\partial u_j}{\partial x_j} - \psi_{ij}$. The macro gradient of micro-deformation, also called the micro-deformation gradient, is called $\varkappa_{ijk} = \partial_i \psi_{jk}$. The stress corresponding to the strain ϵ_{ij} is, via differentiation of the strain energy W, the Cauchy stress $\tau_{ij} = \frac{\partial W}{\partial \epsilon_{ij}}$. The stress corresponding to the micro-deformation gradient \varkappa_{pqr} is called the double stress $\mu_{ijk} = \frac{\partial W}{\partial \varkappa_{ijk}}$. The first subscript of μ_{ijk} represents the normal to the surface across which the component acts. Double stress refers to pairs of forces per unit area. If the pair gives rise to a moment it includes the couple stress of Cosserat elasticity as shown in Fig. 1. Mindlin [8] provides additional illustrations of the geometry of micro-deformation gradient and double stress.

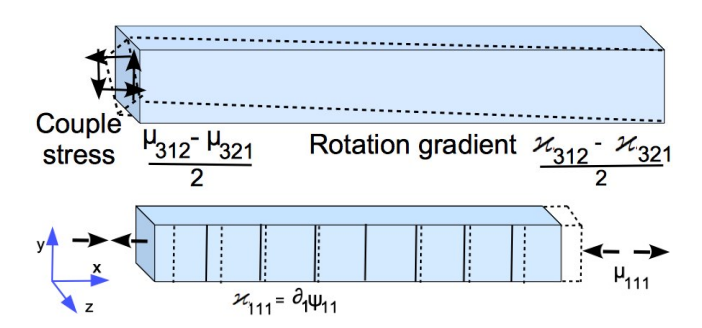


Figure 1: Gradients of micro-deformation \varkappa_{pqr} and corresponding double stress μ_{pqr} , adapted from [8]. Top: Cosserat freedom within micromorphic framework. Bottom: micromorphic freedom for axial compression.

The constitutive equations for the isotropic microstructure theory are for the Cauchy stress, Eq. (1), for the relative stress Eq. (2) and for the double stress, Eq. (3). Here δ_{pq} is the Kronecker delta.

$$\tau_{pq} = \lambda \delta_{pq} + 2G\epsilon_{pq} + g_1 \delta_{pq} \gamma_{ii} + g_2 (\gamma_{pq} - \gamma_{qp}) \tag{1}$$

$$\sigma_{pq} = g_1 \delta_{pq} \epsilon_{ii} + 2g_2 \epsilon_{pq} + b_1 \delta_{pq} \gamma_{ii} + b_2 \gamma_{pq} + b_3 \gamma_{qp}$$
(2)

$$\mu_{pqr} = a_1(\varkappa_{iip}\delta_{qr} + \varkappa_{rii}\delta_{pq}) + a_2(\varkappa_{iiq}\delta_{pr} + \varkappa_{iri}\delta_{pq}) + a_3\varkappa_{iir}\delta_{pq} + a_4\varkappa_{pii}\delta_{qr}$$

$$+a_5(\varkappa_{qii}\delta_{pr} + \varkappa_{ipi}\delta_{qr}) + a_8\varkappa_{iqi}\delta_{pr} + a_{10}\varkappa_{pqr} + a_{11}(\varkappa_{rpq} + \varkappa_{qrp}) +$$

$$a_{13}\varkappa_{prq} + a_{14}\varkappa_{qpr} + a_{15}\varkappa_{rqp}$$

$$(3)$$

Isotropic microstructure / micromorphic elasticity has 18 independent elastic constants (λ , G, g_i , b_i , a_i) compared with 6 for the isotropic Cosserat solid and 2 for the isotropic classical solid.

2.2 Cosserat elasticity

The Cosserat solid is a microstructure solid for which $\psi_{(ij)} = 0$ so $\sigma_{(ij)} = \tau_{ij}$ and $\mu_{i(jk)} = 0$. The Cosserat couple stress is $\mu_{i[jk]}$. The antisymmetric Cosserat relative stress $\sigma_{[ij]}$ can be regarded as an antisymmetric part of an asymmetric stress τ_{ij} . In microstructure elasticity the Cauchy stress τ_{ij} is considered to be symmetric and the antisymmetric part is considered to be part of the asymmetric relative stress σ_{ij} .

In Cosserat elasticity using symbols of the micropolar form [7], the total stress, called σ_{ij} , can be asymmetric. The moment from the antisymmetric part is balanced by a couple stress, m_{ij} . The antisymmetric part of the stress is related to local rotations: $\sigma_{ij}^{antisym} = \kappa e_{ijk}(r_k - \phi_k)$ in which κ is an elastic constant, ϕ_k is the micro-rotation of points, e_{ijk} is the permutation symbol, and $r_k = \frac{1}{2}e_{kij}u_{j,i}$ is the macro-rotation based on the antisymmetric part of the gradient of displacement u_j . The constitutive equations for linear isotropic Cosserat (micropolar) elasticity [7] are as follows.

$$\sigma_{ij} = 2G\epsilon_{ij} + \lambda \epsilon_{kk} \delta_{ij} + \kappa e_{ijk} (r_k - \phi_k) \tag{4}$$

$$m_{ij} = \alpha \phi_{k,k} \delta_{ij} + \beta \phi_{i,j} + \gamma \phi_{j,i} \tag{5}$$

Elastic constants λ and G have the same meaning as in classical elasticity; G is the shear modulus. Elastic constants α , β , γ incorporate sensitivity to gradients of micro-rotation. Elastic constant κ quantifies the coupling between micro and macro rotation fields. Observe that μ as used in ref. [7] is not the shear modulus; such usage of symbols can cause problems [20].

Technical constants, derived from these elastic constants are beneficial for physical insight. They include the shear modulus G and the following.

Young's modulus

$$E = \frac{G(3\lambda + 2G)}{\lambda + G} \tag{6}$$

Poisson's ratio

$$\nu = \frac{\lambda}{2(\lambda + G)} \tag{7}$$

characteristic length, torsion

$$\ell_t = \sqrt{\frac{\beta + \gamma}{2G}} \tag{8}$$

characteristic length, bending

$$\ell_b = \sqrt{\frac{\gamma}{4G}} \tag{9}$$

coupling number

$$N = \sqrt{\frac{\kappa}{2G + \kappa}} \tag{10}$$

polar ratio

$$\Psi = \frac{\beta + \gamma}{\alpha + \beta + \gamma} \tag{11}$$

Size effects are predicted to occur in the bending [21] or torsion [22] of Cosserat solids but not in compression [22].

2.3 Relaxed micromorphic theory

Relaxed micromorphic elasticity [11] has some of the freedom of microstructure elasticity. Two new notations were used. It incorporates Cosserat freedom and two additional elastic constants for a total of eight. The torsion problem [23] was solved for this theory. The uniaxial extension problem was recently analyzed for the relaxed micromorphic continuum and other generalized continua including the Cosserat solid and the void elasticity solid [25]. Size effects are predicted for tension or compression of micromorphic or void solids but not for Cosserat solids. Boundary conditions for size effects in compression are that both displacement and micro-distortion are fixed at the ends. The relaxed micromorphic theory also includes freedom corresponding to a_4 and other a_j in the notation of microstructure elasticity. That freedom allows size effects in compression. Size effects were also predicted for the compression of void solids. No size effects occur in the compression of Cosserat solids, consistent with the analysis in [22].

2.4 Interrelation among symbols

Different notations used for Cosserat elasticity were compared [6]. The Cosserat coupling constant in Eq. (4) is $\kappa = 2\beta$ in the symbols of Mindlin [5]. This constant governs the coupling between micro and macro rotations as well as the magnitude of effects predicted. Correspondences between symbols used for microstructure elasticity [8] and those used by Mindlin for Cosserat elasticity were provided in ref. [5]. Mindlin's Cosserat $\beta = \frac{1}{2}(b_2 - b_3)$ in microstructure elasticity. So the Cosserat coupling constant in Eq. (4) is $\kappa = (b_2 - b_3)$ in microstructure elasticity.

The Cosserat constants associated with rotation gradient sensitivity [5] are linear combinations of several of the microstructure elasticity a coefficients including a_{10} and a_{13} . The relaxed micromorphic theory [24] also contains $\frac{1}{2}(b_2 + b_3)$ within the constant called μ_{micro} .

Referring to Fig. 1 (Fig. 2 in Mindlin 1964), for a compression test with a fixed end condition, the double stress component in the x direction in terms of several components of corresponding the micro-deformation gradient is

$$\mu_{111} = a_4(\varkappa_{111} + \varkappa_{122} + \varkappa_{133}) + a_{10}\varkappa_{111} + a_{13}\varkappa_{111} + a_{14}\varkappa_{111} + \dots$$
(12)

Terms such as \varkappa_{122} could arise from constraint of the Poisson effect at the end. Such effects were not incorporated in the analysis of compression in the relaxed micromorphic theory which subsumes a set of a_j as a single parameter. Observe also that characteristic lengths can be obtained from the square root of the ratio of any combination of the Mindlin a_j coefficients, Cosserat or micromorphic, divided by a classical modulus.

2.5 Physical interpretation

As for quasi-static effects, referring to Fig. 1, one can envisage Cosserat effects arising from distributed moments transmitted through structural elements in the material. These moments arise from gradients in local rotation which in turn are driven by gradients in macro-rotation that occur in torsion, bending and other heterogeneous deformation fields. There are no rotation gradients in tension or compression, so in compression there are no predicted Cosserat effects.

The double stress in micro-structure elasticity includes pairs of self equilibrated forces as well as pairs of forces that give rise to a moment. Effects of self equilibrated force pairs are expected to decay rapidly in the context of Saint Venant's principle. However it is well known that Saint Venant's

principle fails in a space framework of pin jointed ribs [26] [27] [28]. Truss-like frameworks of ribs subjected to self-equilibrated pairs of forces can exhibit rib forces that propagate the full length of the framework, provided the framework is one or two cells wide. Lattice structures and metamaterials might be expected to exhibit micromorphic effects on such a basis. The micromorphic effects that are predicted in compression, including size effects and a nonuniform strain distribution, are driven by a fixed boundary condition on both displacement and micro-distortion at the ends.

Size effects in Cosserat solids [22] can tend to infinity as specimen thickness tends to zero for the limit $N \to 1$. Incorporation of the micromorphic / microstructure freedom [23], specifically $\frac{1}{2}(b_2 + b_3)$, can ameliorate this effect. The limit $b_j \to \infty$ in microstructure elasticity has been described as microhomogeneous [8]; the local degrees of freedom become fully coupled to the macroscopic deformation. The material can nevertheless be strongly nonclassical. The micro-deformation contains an asymmetric part corresponding to the Cosserat micro-rotation and a symmetric part called the micro-strain which can differ from the macroscopic strain. In the Cosserat theory, the relative stress is the antisymmetric part of the stress. In the Cosserat case, this limit corresponds to $\kappa \to \infty$ or $N \to 1$, associated with strong effects provided the specimen is not too much larger than the characteristic length.

As for dynamic effects, Cosserat elasticity in its micropolar variant predicts dispersion of shear waves [7] but no cut off effects and no dispersion of longitudinal waves. Micro-structure / micro-morphic elasticity incorporates sufficient freedom in a continuum approach to allow dispersion of longitudinal waves and cut-off frequencies [8]. The wave velocity can decrease with frequency. The micro-structure elasticity theory gives the angular frequency ω for micro-vibration for waves in equivoluminal extensional modes as

$$\omega^2 = \frac{3(b_2 + b_3)}{\rho d^2} \tag{13}$$

with ρ as density, b_2 and b_3 as nonclassical elastic constants and d as a microstructure size. For a dilatational mode, $3(b_2+b_3)$ is replaced by $3(3b_1+b_2+b_3)$. The elastic constants b_1 , b_2 and b_3 link the relative stress with the relative deformation (the difference between the macro-displacement gradient and the micro-deformation) as given in Eq. (2).

To relate experimental results with micro-structure elasticity one may define [29] a dimensionless measure associated with a cut off frequency.

$$\Lambda^2 = \frac{\omega_c^2 \rho d^2}{3G} \tag{14}$$

with G as the shear modulus, ρ as the density, d as the cell size and ω_c as the observed cut-off angular frequency. So identifying the frequency in Eq. (13) with the cut-off frequency,

$$\Lambda^2 = \frac{3(b_2 + b_3)}{G}. (15)$$

By analogy with Eq. (10) for the Cosserat coupling number N, and recalling $\kappa = (b_2 - b_3)$ one may define

$$N_{micro} = \sqrt{\frac{b_2 + b_3}{2G + (b_2 + b_3)}}. (16)$$

The range for stability for N_{micro} as for N, is from zero to 1. Incorporating Eq. (15),

$$N_{micro} = \sqrt{\frac{\Lambda^2}{6 + \Lambda^2}}. (17)$$

3 Experiments

3.1 Cosserat effects

Cosserat effects are by now well known via bending and torsion size effects in bone [30], in a low density closed cell foam [31], in honeycomb [32], in open cell foam [33], in negative Poisson's ratio foam [34], in an isotropic dense closed cell foam [35], and in designed polymer lattices [37]. Dynamic effects were explored in a non-cohesive granular material comprised of metal spheres [38]. For the dense foam, cross comparisons between torsion and bending size effects as well as warp inferences confirmed the Cosserat interpretation. Asymmetry of the stress has been demonstrated by observing displacement of a notch at the corner of a square cross section bar in torsion [33] [39]. This displacement cannot occur in classically elastic materials because the symmetry of the stress implies stress, hence strain, are zero at the corner. Asymmetry of the stress was also inferred from reduction of warp of square cross section bars in torsion [40]. Cosserat effects also cause sigmoid bulge in the lateral surfaces of bars in bending as shown by analysis [41] and observed in experiments [41] [42].

3.2 Comparison of size effects: compression and torsion

In the following size effect experiments, the ends were bonded to a stiff substrate so the boundary conditions for micromorphic effects are satisfied. Moreover, the ratio of length to width was maintained constant to prevent restraint of Poisson effects from becoming a confounding variable.

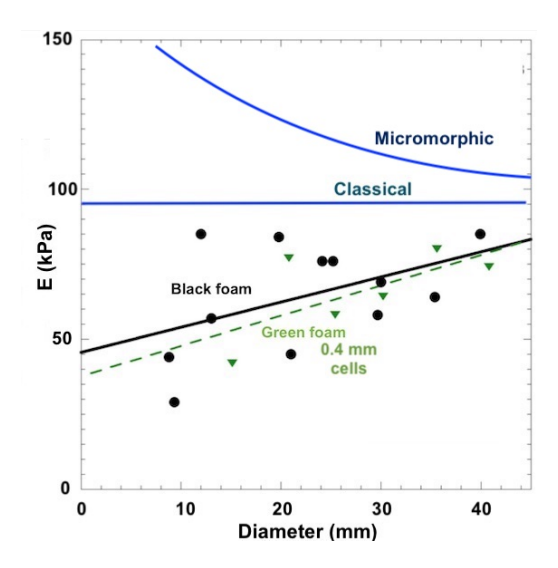


Figure 2: Compression size effects in open cell polymer foams: Young's modulus E vs. diameter. Foams were black foam with 1.2 mm cells and green foam with 0.4 mm cells, adapted from [33]. For a classical solid with no surface effects, the compressive modulus is independent of diameter. For a micromorphic solid, the effective compressive modulus increases as diameter becomes small.

Open cell reticulated foams with 0.4 mm diameter cells exhibit a stiffening size effect in torsion (more than a factor 6) and bending (about a factor 4.8) [33] due to Cosserat freedom but a softening size effect in compression (Figure 2). The softening effect is due to incomplete cells at the surface, a well known effect [43]. This dominates any size effects that might occur due to generalized continuum phenomena associated with the micromorphic theory. Such size effects must entail greater stiffness for smaller diameter, the opposite of the experimental trend in Figure 2. Negative Poisson's ratio foams also exhibit a stiffening size effect in torsion (more than a factor 8) and bending (more than a factor

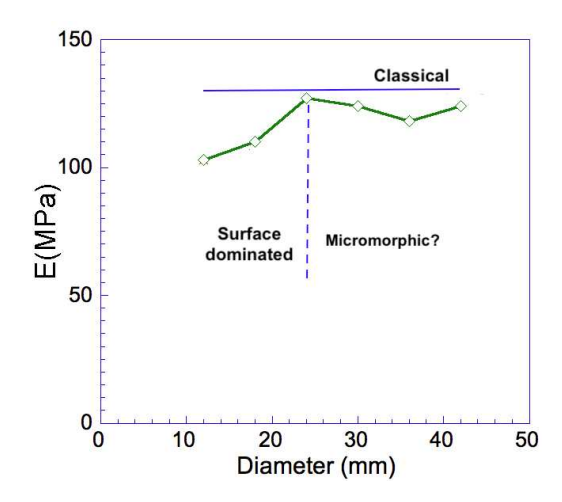


Figure 3: Compression size effects in non-chiral gyroid lattice, adapted from [45]. Young's modulus E vs. diameter.

17) [34] associated with Cosserat freedom but compression tests on these foams revealed no consistent dependence on diameter.

Dense closed cell foam [35] exhibits smaller Cosserat size effects of about a factor 1.35 in torsion and bending. This foam was studied for cut-off frequencies (see below) but size effects in compression were not explored.

The gyroid lattice had a surface wall thickness of 0.4 mm and a cell size of 6 mm. It exhibits a stiffening size effect of 20% to 40% in torsion and about 20% in bending [45]. Results are consistent with a Cosserat coupling number N=1. There is a small stiffening effect, about 5%, in compression of the non-chiral gyroid [45]. At smaller diameters there is a softening effect consistent with a known role [43] for incomplete cells at the surface. The region dominated by surface effects is to the left of the vertical dash line in Figure 3. The chiral gyroids exhibit nonclassical squeeze-twist coupling. Chiral gyroids exhibit size effects in compression (not shown) by virtue of their chirality as can be explained via Cosserat elasticity without recourse to micromorphic elasticity.

Size effects in Cosserat elasticity can diverge as specimen thickness tends to zero [22]; this has been considered to be a motivation to add additional micromorphic terms. However in size effect experiments one cannot allow thickness to tend to zero. The thinnest specimen can be no thinner than one cell (in a cellular solid) or one fiber volume element (in a fibrous solid). For some materials, experimental considerations dictate a minimum thickness of multiple cells. No torsion or bending size effect experiment thus far requires more freedom than that provided in Cosserat elasticity. However, local dilatation [44] was observed in cells of metal foam in compression.

Evidence for micromorphic effects, including reduced micromorphic and void theory, in static size effect experiments is absent in the case of foams and rib lattices and minimal in the case of the gyroid lattice. Such effects may occur in other materials.

3.3 Wave dispersion and cut-off

Longitudinal wave dispersion has been measured in foams [36] and in rib lattices [37]. A resonance method was used. Bars of material were supported at the center and were excited into vibration. Progressively smaller specimens were studied to determine resonant frequency vs. inverse specimen length. The curves obtained can also be expressed as angular frequency $\omega = 2\pi f$ vs. wave number $k = 2\pi/\lambda$. Longitudinal wave dispersion in polymer foams reveal cut off frequencies and approach to

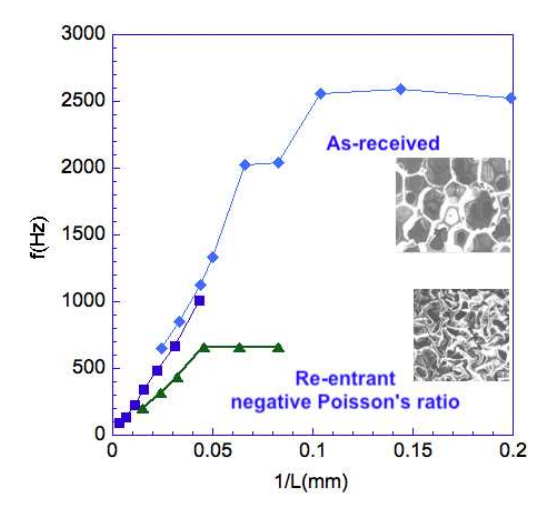


Figure 4: Elastic wave dispersion in a polyester foam, adapted from [29]. Resonant frequency f vs. inverse of specimen length L. The specimen length is $L = \lambda/2$ for the fundamental resonance. Inset: images of foam structure. The cell size was 0.5 mm for as received foam and 0.35 mm for re-entrant negative Poisson's ratio foam.

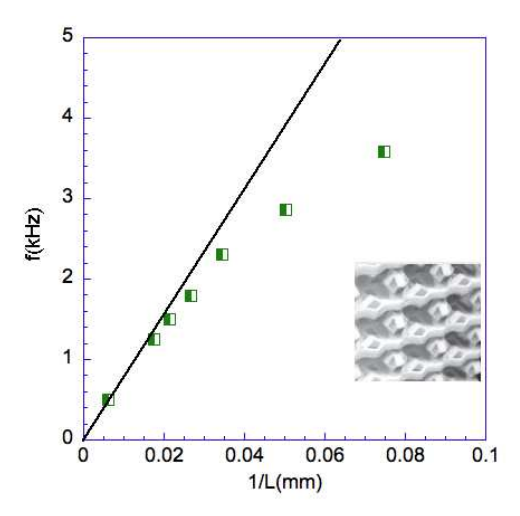


Figure 5: Elastic wave dispersion in a polymer lattice [37] with designed hollow ribs. Resonant frequency f vs. inverse of specimen length L. The specimen length is $L = \lambda/2$ for the fundamental resonance. Inset: image of lattice structure; the cell size is 9 mm in the longitudinal direction.

a horizontal asymptote as shown in Figure 4. The shortest specimens were many cells long. Figure 5 shows dispersion in a polymer lattice [37] designed to exhibit strong nonclassical Cosserat behavior (size effects exceeding a factor of 30) in the quasi-static regime. The black solid line shows the classical asymptote for long wavelength. The smallest specimen was one cell in length. The polymer lattice displays, in Figure 5, a pronounced roll off of the velocity. Even so, the curve did not approach a horizontal asymptote. Cut-off of wave transmission nevertheless occurs.

For compliant open cell foams, dispersion is shown in Figure 4. Referring to Eq. (14), Λ was 0.089 for as-received polyester foam of conventional structure and cell size 0.5 mm, and 0.03 for re-entrant polyester foam with a negative Poisson's ratio.

A dense polyurethane foam was found to be Cosserat elastic [35]. Ultrasonic experiments via the pulse wave transmission method disclosed nearly isotropic behavior within about 7%. Cut-off frequencies were not explored, but waves were transmitted with frequency as high as 1 MHz. Further ultrasonic measurements in the present effort disclosed an upper frequency limit of 1.5 MHz. Incorporating the shear modulus G = 109 MPa, the density, 340 kg/m^3 , the largest cell size 0.15 mm, then $\Lambda = 1.45$.

The strongly nonclassical polymer lattice [37] was Cosserat elastic. It had a density of 0.16 g/cm^3 ; the shear modulus was G = 1.1 MPa and the cell size was d = 9 mm. For a cut-off frequency f = 4 kHz, $\Lambda = 1.6$ for the polymer lattice. Ultrasonic signals from 50 kHz to 1 MHz were input to gyroid specimens. Transmitted signals were too small to measure, so no cut-off frequency is reported. Because the gyroid specimens had a large cell size of 6 mm, it is likely that the dispersion and cut-off occur in the acoustic range, too low for ultrasonic tests to probe.

4 Discussion

Because Λ was associated with a nonclassical rigidity of the unit cell in comparison with the bulk material, the flexible foams may be regarded as having compliant unit cells compared with the lattices and compared with the dense foam. The overall modulus of the material is incorporated in the calculation of Λ , so the compliance of the material is not responsible for the difference.

As for coupling constants, the micromorphic coupling constant N_{micro} was obtained from wave cut-off via Eq. (17). The Cosserat coupling constant (Eq. (10)) N was obtained from size effects in torsion and bending. Cosserat constants including N were corroborated by inferences of warp in torsion of square cross section bars of dense foam, by direct measurements of nonclassical warp in low density open cell foam [40], and by measurements of nonclassical sigmoid lateral bulge in bending in low density foam and in dense foam [41] [42].

Dense polymer foam had $N_{micro} = 0.7$. In comparison, N = 0.15. For the dense foam, a small value of N is associated with modest size effects of about a factor 1.35. The value of N was corroborated by inferences of warp of square cross section bars. For the strongly nonclassical lattice, $N_{micro} = 0.55$. In comparison N = 1 for this lattice. For low density polyester foam of conventional structure $N_{micro} = 0.036$ and for negative Poisson's ratio foam made from that, $N_{micro} = 0.012$. The open cell foams in [29] were not studied for Cosserat size effect but similar foams [33] exhibited N = 0.99. All of these materials exhibited Cosserat characteristic lengths on the order of or greater than the cell size.

As for physical interpretation, N represents the degree of coupling between micro-rotation of points and the macro-rotation associated with motion of nearby points in Cosserat elasticity. N_{micro} represents the degree of coupling between a component of micro-strain of points and the macro-strain associated with motion of nearby points in micromorphic elasticity. By contrast, the characteristic length scale at which nonclassical effects occur is given by the square root of a combination of micromorphic a coefficients and a classical elastic modulus. In the symbols of Cosserat elasticity, Eq. (8) and Eq. (9) give characteristic lengths in terms of Cosserat constants β and γ .

Although N_{micro} is predicted to moderate the size effects in torsion of slender specimens compared with the predictions of Cosserat elasticity, a Cosserat interpretation was found to suffice for all such size effect studies conducted to date. It is possible that effects of N_{micro} would appear if specimens were made more slender than was practicable in the experiments.

5 Conclusions

Cut off frequencies in dynamic experiments provide evidence for micromorphic effects associated with microstructure constants $(b_2 + b_3)$, expressed as N_{micro} . This freedom does not suffice to impose itself

on the interpretation of quasi-static size effect experiments for which a Cosserat interpretation suffices. Compressive size effects in foam were dominated by softening due to incomplete cells at the surface. The associated micromorphic a coefficients are therefore much smaller than those for Cosserat elasticity as revealed by torsional and bending size effects. Compressive size effects in a non-chiral gyroid lattice were small, suggesting a slight micromorphic effect.

The author gratefully acknowledges support of this research by the National Science Foundation via Grant No. CMMI -1906890. I thank Professor Rizzi and Professor Neff for discussions on the reduced micromorphic theory.

References

- [1] Sokolnikoff, I. S., Theory of Elasticity, Krieger; Malabar, FL, 1983.
- [2] Timoshenko, S.P., History of Strength of Materials, Dover, NY, 1983.
- [3] W. Koiter, Couple stresses in the theory of elasticity: I and II, Proc. Koninkl. Ned. Akad. Wetensch. Ser. B 67, 17-44 (1964).
- [4] E. Cosserat and F. Cosserat, Theorie des Corps Deformables, Hermann et Fils, Paris (1909).
- [5] R. D. Mindlin, Stress functions for a Cosserat continuum, Int. J. Solids Structures, 1, 265-271 (1965).
- [6] R. D. Mindlin, Stress functions for Cosserat elasticity, Int. J. Solids Structures, 6, 389-398 (1970).
- [7] A. C. Eringen, Theory of micropolar elasticity. In Fracture Vol. 1, 621-729 (edited by H. Liebowitz), Academic Press, New York (1968).
- [8] Mindlin, R. D., Micro-structure in linear elasticity, Arch. Rational Mech. Analy, 16, 51-78, (1964).
- [9] Cowin, S. C. and Nunziato, J. W., Linear elastic materials with voids, J. Elasticity 13 125-147 (1983)
- [10] Eringen, A. C., Theory of thermo-microstretch elastic solids, Int. J. Engng. Sci., 28 (12)1291-1301, 1990.
- [11] P. Neff, I. Ghiba, A. Madeo, L. Placidi, and G. Rosi, A unifying perspective: the relaxed linear micromorphic continuum, Continuum Mechanics and Thermodynamics 26.5, 639-681 (2014).
- [12] A. Askar and A. S Cakmak, A structural model of a micropolar continuum, Int. J. Engng. Sci. 6, 583-589 (1968).
- [13] T. Tauchert, A lattice theory for representation of thermoelastic composite materials, Recent Advances in Engineering Science, 5, 325-345 (1970).
- [14] D. Bigoni and W. J. Drugan, Analytical derivation of Cosserat moduli via homogenization of heterogeneous elastic materials, J. Appl. Mech., **74**, 741-753 (2007).
- [15] Prall, D., and Lakes, R.S., Properties of a chiral honeycomb with a Poisson's ratio of -1. Int. J. of Mech. Sci. 39(3), 305-314 (1997).
- [16] Spadoni A., and Ruzzene M., Elasto-static micropolar behaviour of a chiral auxetic lattice. J. Mech. Phys. Solids 60, 156-171 (2012).
- [17] S. Minagawa, Arakawa, K., Yamada, M., Diamond crystals as Cosserat continua with constrained rotation, Physica Status Solidi A 57, 713-718, (1980).
- [18] Y. Chen and J. D. Lee, Determining material constants in micromorphic theory through phonon dispersion relations, International Journal of Engineering Science 41 871-886 (2003)
- [19] T. Dillard, S. Forest and P. Ienny, Micromorphic continuum modelling of the deformation and fracture behaviour of nickel foams, European Journal of Mechanics A, Solids, 25, 526-549, 2006.
- [20] S. C. Cowin, An incorrect inequality in micropolar elasticity theory, Zeitschrift für Angewandte Mathematik und Physik, 21, 494-497, 1970.
- [21] Krishna Reddy, G. V. and Venkatasubramanian, N. K., On the flexural rigidity of a micropolar elastic circular cylinder, J. Applied Mechanics 45, 429-431, 1978.
- [22] Gauthier, R. D. and W. E. Jahsman, 1975, A quest for micropolar elastic constants. J. Applied Mechanics, 42, 369-374.
- [23] G. Rizzi, G. Hutter, H. Khan, I. D. Ghiba, A. Madeo, and P. Neff, Analytical solution of the cylindrical torsion problem for the relaxed micromorphic continuum and other generalized continua (including full derivations), (arXiv:2104.11322) Mathematics and Mechanics of Solids, 27, (3) (2021). https://doi.org/10.1177/10812865211023530
- [24] G Rizzi, H. Khan, I. D. Ghiba, A. Madeo, and P. Neff, Cosserat micropolar elasticity: classical Eringen vs. dislocation form, https://arxiv.org/abs/2206.02473v1
- [25] G Rizzi, I. D. Ghiba, A. Madeo, and P. Neff, Analytical solution of the uniaxial extension problem for the relaxed micromorphic continuum and other generalized continua (including full derivations), Arch. Appl. Mech. (2021). https://doi.org/10.1007/s00419-021-02064-3

- [26] N. J. Hoff, The applicability of Saint Venant's principle to airplane structures, Journal of Aeronautical Science 12, 455-460 (1945)
- [27] Y. C. Fung, Foundations of Solid Mechanics, Prentice Hall, N.J. (1968).
- [28] N. G. Stephen and P. J. Wang, On Saint Venant's principle in pin jointed frameworks, Int. J. Solids Structures, 33, 79-97 (1996).
- [29] Chen, C. P. and Lakes, R. S., Dynamic wave dispersion and loss properties of conventional and negative Poisson's ratio polymeric cellular materials, Cellular Polymers, 8(5), 343-359 (1989).
- [30] Yang, J. F. C., and Lakes, R. S., Experimental study of micropolar and couple stress elasticity in bone in bending, Journal of Biomechanics, 15, 91-98, (1982).
- [31] Lakes, R. S., Size effects and micromechanics of a porous solid, J. Materials Science, 18 2572-2581, (1983).
- [32] R. Mora and A. M. Waas, Measurement of the Cosserat constant of circular cell polycarbonate honeycomb, Philosophical Magazine A, 80, 1699-1713 (2000).
- [33] Rueger, Z. and Lakes, R. S., Experimental Cosserat elasticity in open cell polymer foam, Philosophical Magazine, 96 (2), 93-111, (2016).
- [34] Rueger, Z. and Lakes, R. S., Cosserat elasticity of negative Poisson's ratio foam: experiment, Smart Materials and Structures, 25 054004 (8pp) (2016).
- [35] Z. Rueger and R. S. Lakes, Experimental study of elastic constants of a dense foam with weak Cosserat coupling, J. Elasticity, 137, 101-115, (2019).
- [36] Chen, C. P. and Lakes, R. S., Dynamic wave dispersion and loss properties of conventional and negative Poisson's ratio polymeric cellular materials, Cellular Polymers, 8(5), 343-359 (1989).
- [37] Rueger, Z. and Lakes, R. S., Strong Cosserat elasticity in a transversely isotropic polymer lattice, Phys. Rev. Lett., 120, 065501 (2018).
- [38] A. Merkel and V. Tournat, Experimental evidence of rotational elastic waves in granular phononic crystals, Phys. Rev. Lett., **107**(22), 225502 (2011).
- [39] Lakes, R. S., Gorman, D., and Bonfield, W., Holographic screening method for microelastic solids, J. Materials Science, 20, 2882-2888 (1985).
- [40] Lakes, R. S., Reduced warp in torsion of reticulated foam due to Cosserat elasticity: experiment, Zeitschrift fuer Angewandte Mathematik und Physik (ZAMP), 67(3), 1-6 (2016).
- [41] Lakes, R. S. and Drugan, W. J., Bending of a Cosserat elastic bar of square cross section theory and experiment, Journal of Applied Mechanics, 82(9), 091002 (2015). (8 pages).
- [42] R. S. Lakes, Cosserat shape effects in the bending of foams, Mechanics of Advanced Materials and Structures, Published online: 14 Jun 2022 doi link https://doi.org/10.1080/15376494.2022.2086328
- [43] Brezny, R. and Green, D. J., Characterization of edge effects in cellular materials, J. Materials Science, 25 (11), 4571-4578 (1990)
- [44] A. Burteau, F. NGuyen, J.D. Bartout, S. Forest, Y. Bienvenu, S. Saberi and D. Naumann, Impact of material processing and deformation on cell morphology and mechanical behavior of polyurethane and nickel foams, International Journal of Solids and Structures, 49, 2714-2732, 2012.
- [45] D. R. Reasa and R. S. Lakes, Nonclassical chiral elasticity of the gyroid lattice, Phys. Rev. Lett. 125, 205502, (2020).
- [46] T. DeValk and R. S. Lakes, Poisson's ratio and modulus of the gyroid lattice, Physica Status Solidi B 258 (12) 2100081 (2021).